

Chemical and Theoretical Studies for Corrosion Inhibition of Magnesium in Hydrochloric Acid by Tween 80 Surfactant

Salah Eid¹, Walid M. I. Hassan^{2,*}

¹Chemistry department, Faculty of science, Benha University, Benha, Egypt

²Chemistry department, Faculty of science, Cairo University, Giza, Egypt

*E-mail: walid_m76@yahoo.com

Received: 26 May 2015 / Accepted: 23 July 2015 / Published: 26 August 2015

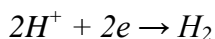
The aim of this paper is to study the corrosion inhibition of magnesium in hydrochloric acid by using tween 80 surfactant. The inhibition action of tween 80 was studied using hydrogen evolution and weight loss methods. It was found that the addition of tween 80 surfactant inhibits the corrosion rate. The inhibition action was expounded on the basis of adsorption of tween 80 on the magnesium surface forming a hindrance of mass and charge transfer leading to protect the magnesium surface from the aggressive ions. The values of adsorption thermodynamic parameters were calculated and explained. Moreover, theoretical calculation for the energetic parameters and natural bond orbital charges for the tween 80 have been done using hybrid density functional theory B3LYP. The calculations show that non-homogenous branching in tween 80 is more stable compared to homogenous one by about 0.36 eV which can be related to steric hindrances. The theoretical calculations showed that during the physical adsorption, partial electronic charge are transferred from magnesium surface to LUMO orbital which is localized on the ester group.

Keywords: magnesium, surfactant, Tween 80, corrosion inhibitors, theoretical, DFT.

1. INTRODUCTION

Magnesium is the ninth most abundant element in the world. Magnesium and its alloys have low densities, excellent heat dissipation, good mechanical and electrical properties, and good electromagnetic shield, so, they have been used in many applications [1-5]. The disadvantages of magnesium are its high reactivity and low corrosion resistance [6-9]. The reasons for the high reactivity of magnesium are the high corrosion tendency due to the high electron negative potential, the oxide film forming on surface is not perfect and galvanic corrosion can be happened by impurities or secondary phases [10-11].

The corrosion of magnesium in hydrochloric acid may occur according to the following equations:



The researches on the protection of magnesium by adding corrosion inhibitors is small [12-14]. Many organic surfactants, e.g. tween series, has been used as inhibitor due to their low cost, high inhibition efficiency, low toxicity and easy production [15-16].

The aim of this paper is to study the corrosion inhibition of magnesium in hydrochloric acid using tween 80 surfactant by chemical techniques due to its reliability and cheap equipment required. Experimental evaluation of the inhibition efficiency and theoretical investigation to the mode of adsorption are presented.

2. MATERIALS AND METHODS

Magnesium sheets $50 \times 3.3 \times 0.2$ mm were used for weight loss and hydrogen evolution experiments. Before being used, the magnesium sheet was polished successively with various grades of emery papers until 2500 grad, degreased with acetone and then washed with distilled water. All chemicals used in the present work were pure laboratory grade (BDH) products and were used without further purification. A stock solution of 1×10^{-2} M was prepared from tween 80 (IUPAC name, polyoxyethylene (20) sorbitan monooleate), by accurate weighting and dissolving in distilled water. Also, stock solution of 4 M HCl was prepared. The stock solutions used to prepare the desired concentration by dilution with distilled water. The experiments were carried out at $25 \pm 1^\circ\text{C}$ using thermostat. Plastic clips have been used to prevent magnesium sheets from floating.

All the calculations are performed using Gaussian 09w[17] using B3LYP [18-20]. Two different basis sets were implemented, 3-21G and 6-321G for Tween 80 with $w+x+y+z = 20$ and 1 respectively. The hybrid DFT method, B3LYP contains Becke Three Parameter Hybrid Functionals[18] that uses the non-local correlation provided by the LYP expression,[19] and local correlation by VWN functional III [20]. The geometry optimization process involves using analytical gradients of energy until a stationary point on the potential surface is achieved during this process we did not involve any restrictions on symmetry of the molecule.

3. RESULTS AND DISCUSSION

3.1 Hydrogen evolution studies.

The effect of increasing concentrations of tween 80 surfactant on the hydrogen evolution obtained during the corrosion reaction of magnesium in 0.3 M HCl solution at 298 K was presented in Fig. (1). Table (1) shows the effect of increasing concentrations of tween 80 surfactant on the hydrogen volume, the percentage of inhibition efficiency (%IE) and the amount of surface coverage

(θ) for the corrosion of magnesium in 0.3 M HCl solution after ten minutes. The inhibition efficiency and surface coverage were calculated by using the following equations:

$$\%IE = (1 - V_{Inh}/V_{Free}) \times 100$$

$$\theta = \%IE / 100$$

where V_{Free} and V_{Inh} are the volumes of hydrogen evolved after 10 minutes in absence and presence of the inhibitor, respectively.

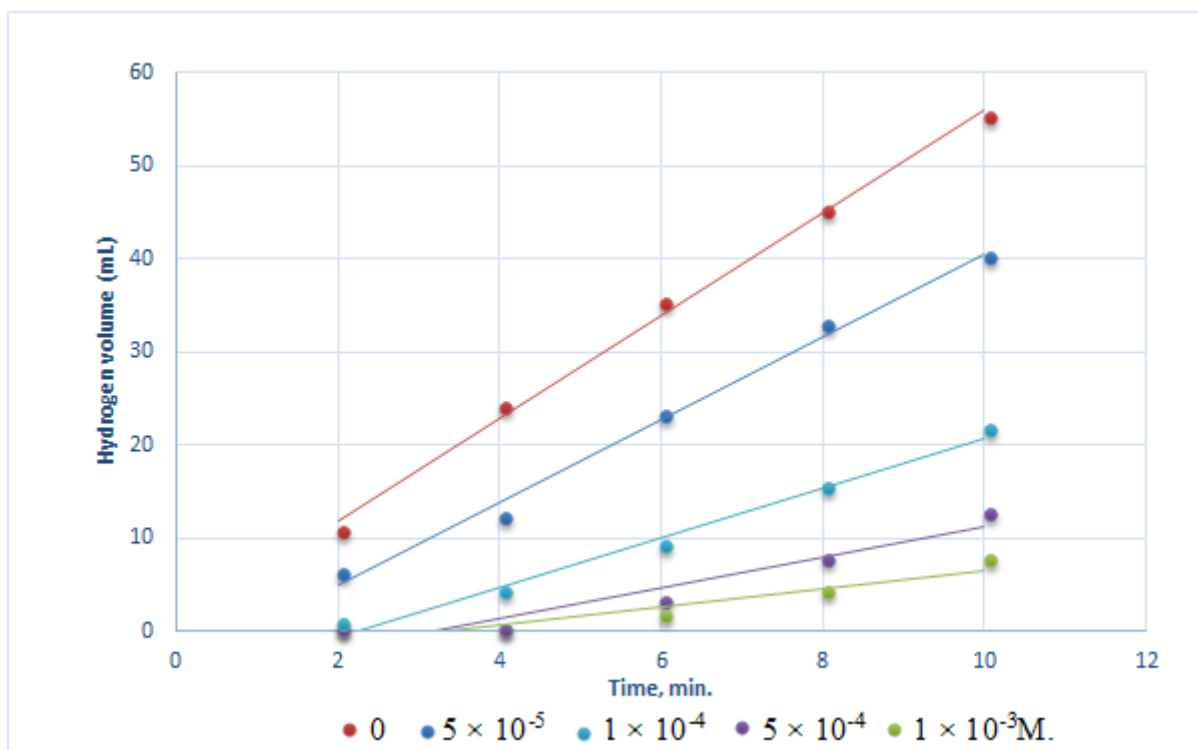


Figure 1. The effect of the addition of various concentrations of tween 80 surfactant on the hydrogen evolution obtained during the corrosion reaction of magnesium in 0.3 M HCl solution at 298 K.

Table 1. The effects of the addition of various concentrations of tween 80 surfactant on the weight of magnesium in 0.3 M HCl solution at 298 K

Type of inhibitor	Inh. Conc. (M)	Hydrogen volume (mL)	IE%	θ
Tween 80	0	55	0	0
	5×10^{-5}	40	27.3	0.273
	1×10^{-4}	21.5	60.9	0.609
	5×10^{-4}	12.5	77.3	0.773
	1×10^{-3}	7.5	86.4	0.864

Inspection of the data reveals that, the hydrogen evolution decreases, while the surface coverage and inhibition efficiency increase with increasing additive concentration. The organic

compound contains oxygen atoms with a lone pair of electrons, which facilitates its adsorption on the magnesium surface. The occurrence of the adsorption of the compound on magnesium surface constitutes barrier for mass and charge transfer, leading to protect the metal surface from the aggressive ions attack [21].

3.2 Weight loss studies.

Table 2. The effect of the addition of various concentrations of tween 80 surfactant on the weight of magnesium in 0.3 M HCl solution at 298 K.

Type of inhibitor	Inh. Conc. (M)	Weight loss (gm)	IE%	θ
Tween 80	0	0.0604	0	0
	5×10^{-5}	0.0444	26.5	0.265
	1×10^{-4}	0.027	55.3	0.553
	5×10^{-4}	0.0162	73.2	0.732
	1×10^{-3}	0.01	83.4	0.834

The effects of increasing concentration of tween 80 surfactant on weight loss, the percentage of inhibition efficiency (%IE) and the amount of surface coverage (θ) for the corrosion of magnesium in 0.3 M HCl solution after ten minutes were given in Table (2). The inhibition efficiency was calculated by using the following equation:

$$\%IE = (1 - W_{Inh}/W_{Free}) \times 100$$

where W_{Free} and W_{Inh} are the weight loss of magnesium after 10 minutes in absence and presence of the inhibitor, respectively. It was found that the weight loss decreases, while surface coverage and inhibition efficiency increase with increasing the tween 80 concentration. The relation between (%IE) and tween 80 concentration was given in Fig. 2.

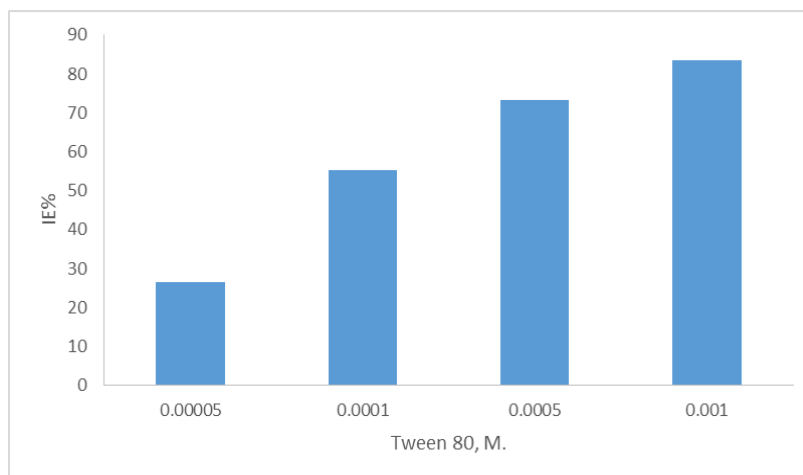


Figure 2. Relation between tween 80 concentrations and its IE% for the magnesium corrosion in 0.3 M HCl

The obtained results from the weight loss measurements is in agreement with the hydrogen evolution measurements.

3.3 Adsorption isotherm

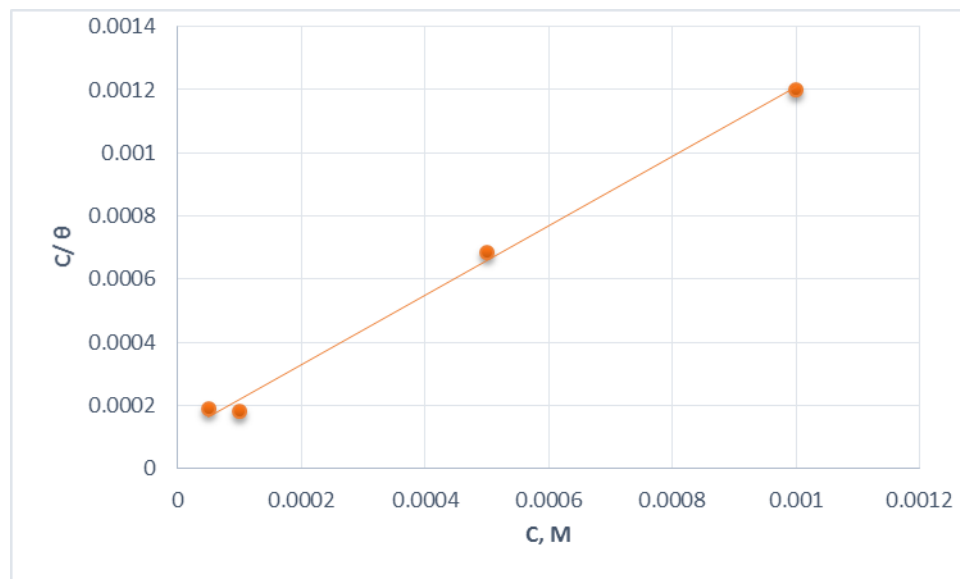


Figure 3. Relation between C/θ and C for corrosion of magnesium in 0.3 M HCl in the presence of tween 80 solution.

The adsorption behavior of tween 80 surfactant on the magnesium surface can be interpreted by finding a suitable isotherm. Many mathematical relationships for the adsorption isotherms has been proposed to fit the experimental data of the present work. The equation that fits our results is Langmuir adsorption isotherm equation which is given by [15]:

$$C/\theta = 1/K + C$$

where K and C are the equilibrium constant of the adsorption process and additive concentration, respectively.

A plot of C/θ against C gave straight line with slope equal unit as shown in fig (3). The equilibrium constant of adsorption, K , is proportional to the standard free energy of adsorption, $\Delta G_{\text{ads}}^{\circ}$, with the following equation [22]:

$$K = 1/55.5 \exp(-\Delta G_{\text{ads}}^{\circ}/RT)$$

where T is the absolute temperature and R is the gas constant ($8.314 \text{ J} \cdot \text{mol}^{-1} \cdot \text{K}^{-1}$).

The equilibrium constant is equal to 10000 and the adsorption free energy of surfactant adsorbed on the surface of magnesium in 0.3 M HCl is equal to $-32.77 \text{ kJ} \cdot \text{mol}^{-1}$. In general, values of $\Delta G_{\text{ads}}^{\circ}$ around $-20 \text{ kJ} \cdot \text{mol}^{-1}$ or lower are consistent with the electrostatic interaction between the charged molecules and the charged metal (physisorption)[23]. Those more negative than $-40 \text{ kJ} \cdot \text{mol}^{-1}$ involve charge sharing or transfer from the inhibitor molecules to the metal surface to form a coordinate type of bond (chemisorption) [24-25]. The calculated values of $\Delta G_{\text{ads}}^{\circ}$ are greater than $-20 \text{ kJ} \cdot \text{mol}^{-1}$ but less than $-40 \text{ kJ} \cdot \text{mol}^{-1}$, indicating that the adsorption of mechanism of tween 80 on

magnesium in 0.3M HCL solution may be a combination of both physisorption and chemisorption [26].

3.4 Thermodynamic calculations

The effect of increasing temperature on the volume of hydrogen evolved from the corrosion of magnesium in 0.3 M HCl in absence and presence 0.001 M tween 80 surfactant after 10 minutes was given in Fig. 4. The data reveals that the rate of corrosion increases as temperature increase.

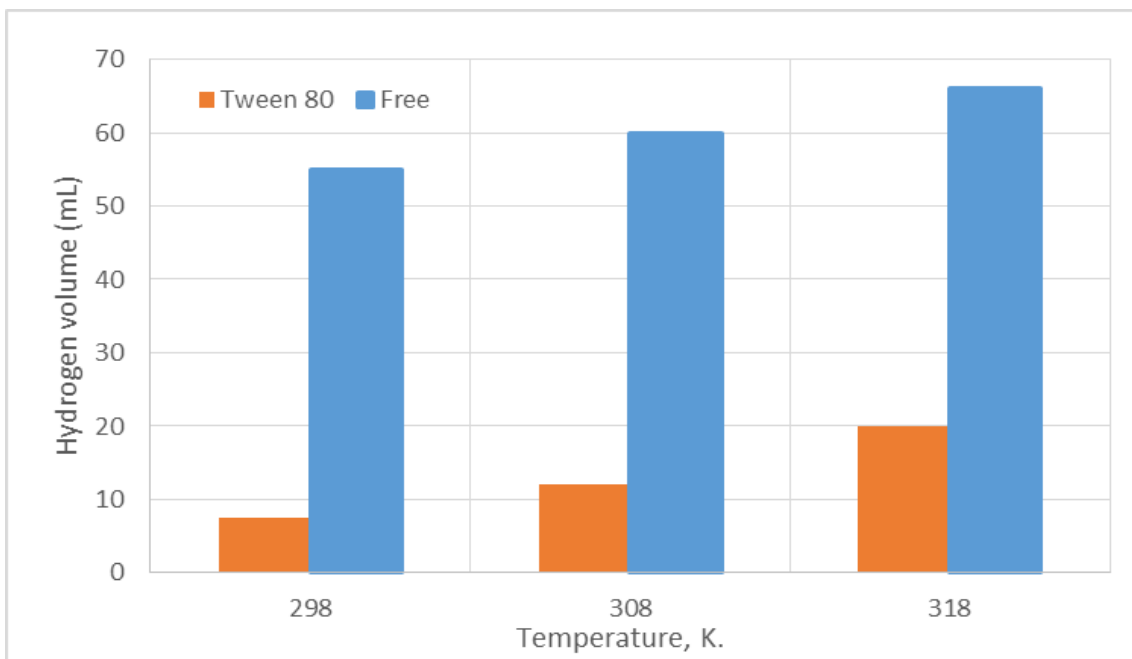


Figure 4. Relation between hydrogen volume and temperature for corrosion of magnesium in 0.3 M HCl in absence and presence of tween 80 solution.

The apparent activation energy E_a for the corrosion of magnesium in 0.3 M HCl in the absence and presence of 0.001 M tween 80 surfactant was calculated using Arrhenius type equation [27]:

$$\log(H_{T_2}/H_{T_1}) = (E_a/2.303R)((1/T_1) - (1/T_2))$$

where A is the Arrhenius pre-exponential factor, T is the absolute temperature, E_a is the apparent activation energy, R is the universal gas constant, H_{T_1} and H_{T_2} are the hydrogen rate (mL/min) which calculated after 10 minutes at temperature T_1 and T_2 , respectively. The values of the activation energies (E_a) were calculated and given in Table (3). This value is higher than the value of obtained for the blank and lower than the threshold value of 80 kJ mol^{-1} required for the mechanism of chemical adsorption. This indicates that the mechanism of adsorption is physical adsorption [27].

From the values of E_a (38.6 kJ mol^{-1}) and $\Delta G_{\text{ads}}^{\circ}$ ($-32.77 \text{ kJ. mol}^{-1}$), physisorption was the major contributor while chemisorption only slightly contributed to the adsorption mechanism [23].

Table 3. The values of adsorption parameters of magnesium in 0.3 M HCl and 0.001 M tween 80 surfactant.

Solution	H ₁ 298 K	H ₂ 318 K	θ ₁ 298 K	θ ₂ 318 K	E _a kJ. mol ⁻¹	Q _{ads} kJ. mol ⁻¹	ΔS _{ads} J. mol ⁻¹ .K ⁻¹
Free	5.5	6.6	-	-	7.18	-	-
Tween 80	0.75	2	0.864	0.70	38.6	-39.5	22.58

The heat of adsorption of the inhibitor was calculated using the following equation [24]:

$$Q_{\text{ads}} = 2.303 R [\log (\theta_2/(1-\theta_2)) - \log (\theta_1/(1-\theta_1))] \times [T_1 T_2 / (T_2 - T_1)]$$

where, θ_1 and θ_2 are the amount of surface coverage at temperature T_1 and T_2 , respectively.

The calculated value of Q_{ads} was recorded in Table 3. It has negative value, so the adsorption of the inhibitor on magnesium surface is exothermic. Also, the negative value indicates that the amount of surface coverage decreased with increase in temperature, supporting the earlier proposed physical adsorption mechanism.

From the calculated values of the free energy and enthalpy change, the entropy for the adsorption of tween 80 on magnesium surface was calculated by the following equation [28]:

$$\Delta S_{\text{ads}}^{\circ} = (\Delta G_{\text{ads}}^{\circ} - \Delta H_{\text{ads}}^{\circ}) / T$$

The value of entropy changes is presented in Table 3. From the results obtained, the entropy of the adsorption has positive value. This is obverse to what would be expected, since adsorption is an exothermic process. Ateya et al. [29] described this case. In this case there are two process happened simultaneously, the adsorption of the inhibitor and desorption of water molecules from the metal surface. Thus, the adsorption process is thought to be exothermic and associated with a decrease in the entropy of the solute, while the obverse is true for the solvent. The thermodynamic values obtained are the sum of the adsorption of organic molecules and desorption of water molecules [30]. So, the gain in entropy is attributed to the rise in solvent entropy [29, 30].

3.5 Molecular Simulation

Tween 80 molecular formula is shown in figure 5a. The energetic parameters of tween 80 were modeled using different possible length combinations for w, x, y and z branches while keeping the total value fixed to 20. The calculated parameters are summarized in table 4. The least stable geometry were obtained when the all the branches are equally distributed (i.e. $w = x = y = z = 5$) by 0.36 eV. Furthermore, Uneven branching is more stable than even branching due to it shows less steric hindrance.

In addition to, the most stable geometry were obtained by having a longer z-branch due to it is far way from other branches which is almost free of steric compared to other branches. The dipole moment increases as the stability decrease with exception of $w=17$ structure.

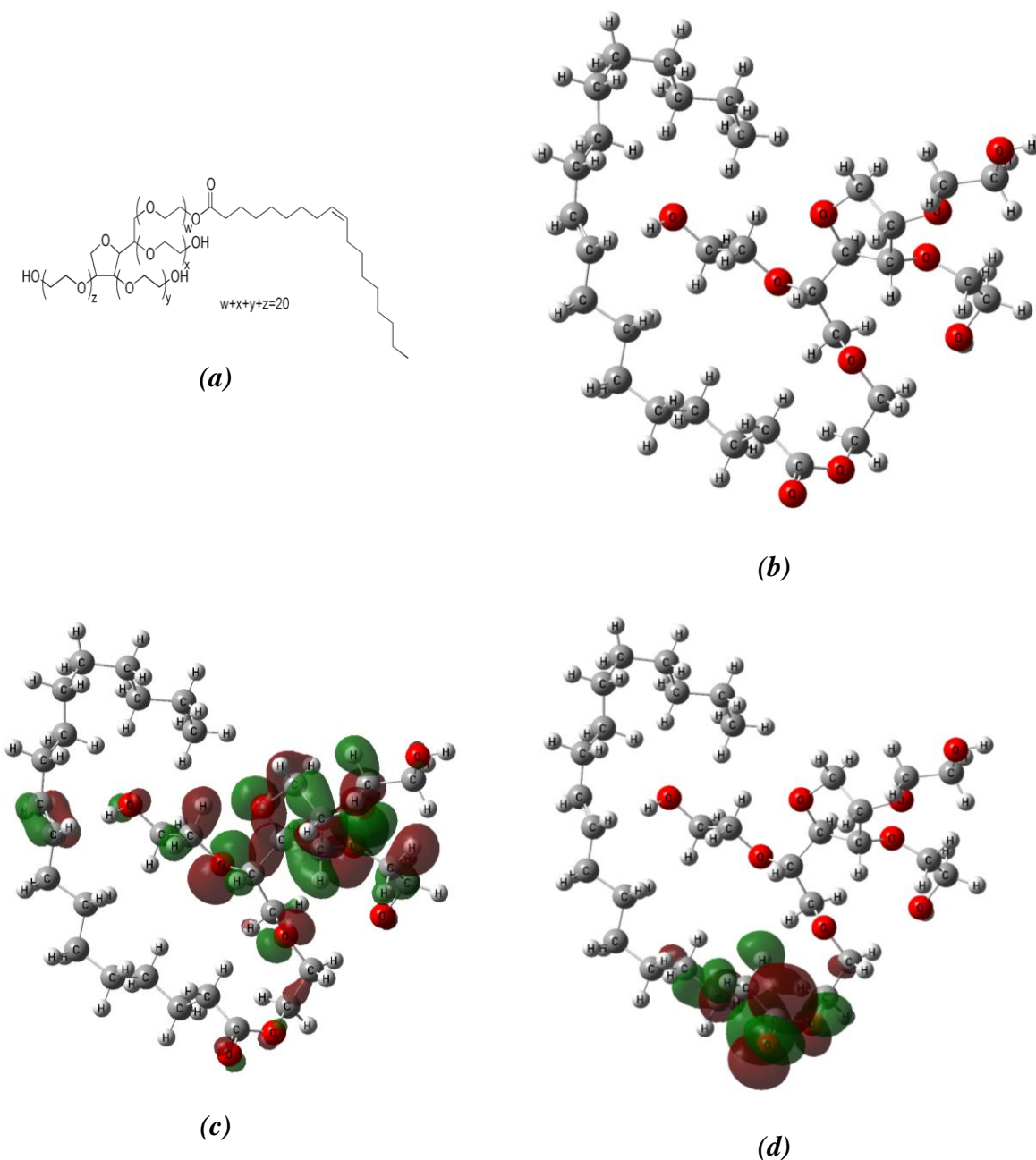


Figure 5. The structure (a), calculated optimized geometry (b), HOMO and LUMO plots (c,d) of Tween 80 using B3LYP and 6-31G as a basis set.

The maximum changes in the energy values of the highest occupied molecular orbital (HOMO), lowest unoccupied molecular orbital (LUMO) and the energy gap ΔE between E_{LUMO} and E_{HOMO} are less than 0.4, 0.2 and 0.5 eV respectively. The lower value of ΔE is usually considered as a measure of higher reactivity, once again the longer w-branch has the lowest ΔE and is expected to show the highest reactivity. The larger size of tween 80 (214 atoms and 716 electrons) forced us to model it using relatively small basis set 3-21G to save the computational power.

Table 4. The total energy in a.u., total energy difference, E_{HOMO} , E_{LUMO} and energy gap in eV for Tween 80.

Basis set	z	y	X	W	E_{Total} , a.u.	ΔE_{Total} , eV	E_{HOMO} , eV	E_{LUMO} , eV	ΔE , eV	μ , Debye
3-21G	17	1	1	1	- 4444.51350105	0.0000	-6.3509	0.5391	6.8899	7.05
3-21G	1	17	1	1	- 4444.50968902	0.1037	-6.4891	0.4264	6.9155	4.46
3-21G	1	1	17	1	- 4444.50746300	0.1643	-6.3950	0.3703	6.7653	3.59
3-21G	1	1	1	17	- 4444.50412866	0.2550	-6.0711	0.3344	6.4056	4.36
3-21G	5	5	5	5	- 4444.50023789	0.3609	-6.2170	0.3260	6.5430	2.61
3-21G	1	1	1	1	-1996.7178585	--	-6.3403	0.5527	6.8929	6.95
6-31G	1	1	1	1	-2007.0863882	--	-6.6850	0.1293	6.8143	5.59

Surprisingly, the smaller theoretical molecule $w = x = y = z = 1$ (102 atoms and 332 electrons) have almost the same energetic parameters as the most stable tween 80 structure with a maximum difference of 0.0136 eV. This suggests that the theoretical tween 80 ($w = x = y = z = 1$) can be satisfactory assumed to be representative to Tween 80 ($w+x+y+z = 20$). This phenomenon might be explained by the fact that longer chain in Tween 80 has a minor effect on its central part due to extremely large distance between the chain terminal end and the center of the molecule. On the other hand, the interaction between different Tween 80 side chains will be of great importance if the material is in crystalline form but not in isolated gas phase. The calculation for theoretical Tween 80 molecule ($w = x = y = z = 1$) at moderate basis set 6-31G were done and the optimized geometry is shown in figure 5b and energetic are summarized in table 1 respectively.

The energy of E_{HOMO} , E_{LUMO} and ΔE do not show any apparent change at 6-31G basis set compared to the ones obtained at 3-21G basis set. In the following sections, we will discuss the theoretical tween 80 results and we will refer to it as tween 80 for simplicity.

The optimized geometry of tween 80 shows that w-branch is folded towards the tetrahydrofuran ring and may be interacting with y-branch. On the other hand, the x and y branches are almost non-interacting with other branches. The HOMO and LUMO plots of Tween 80 are shown in Figure 5c and 5d respectively. The HOMO plot is de-localized over the whole molecule with exception of aliphatic CH_2 chain parts and mainly on tetrahydrofuran, nearby ethoxy groups and ethene bond. On the other hand, the LUMO is localized on the ester group on the w-branch. The adsorption process will mainly be interaction of occupied orbital of one moiety and unoccupied moiety from the other. Since, E_{HOMO} is often associated with the electron-donating ability of a molecule, while, E_{LUMO} indicates the ability of the molecule to accept electrons [31]. The more negative E_{HOMO} indicates lower donating tendency since electrons will be more attracted to the nucleus and Ionization potential is usually taken as $-E_{\text{HOMO}}$. On the other hand, since $\text{EA} = -E_{\text{LUMO}}$, the more positive E_{LUMO} indicates larger affinity for electrons. In our calculation E_{HOMO} is much more negative than positivity of E_{LUMO} which indicates a greater tendency to accept electron than to donate it. The E_{HOMO} and E_{LUMO} of optimized magnesium

dimmer using 6-31G/B3LYP method are -4.9345, -1.3227 eV respectively. The calculated E_{HOMO} and E_{LUMO} of magnesium dimmer, may lead to the conclusion, that physical adsorption will be formed by partial charge movement from magnesium surface to the tween 80 LUMO. Relatively low ΔE gives good inhibition efficiencies because it will be more reactive and it may react faster with the surface results in greater passivation [32, 33]. The larger value of the dipole moment, μ will favor the accumulation of inhibitor molecules on the metallic surface [31, 34].

Further investigation of the interaction between tween 80 and surface can be done by analyzing the natural bond orbital charges. The most negative atoms are terminal heavy atoms which are Oxygen in OH terminal branches (x, y and z); and carbon in w-branch. The charges at that terminal heavy atoms are -0.758, -0.772, -0.772 and -0.695 for z, y, x, w branches respectively. The most positive atomic charge in tween 80 is +0.785 e on the carbon of the ester group. These data, in combinations of the HOMO and LUMO plots and energy further suggests that donated partial electron charges from magnesium surface to the LUMO localized on the ester group.

4. CONCLUSIONS

- The addition of tween 80 surfactant inhibits the corrosion of magnesium and the inhibition incidence depends upon the concentration of the surfactant.
- The adsorption of tween 80 on magnesium surfaces in HCl solution follows Langmuir isotherm.
- The inhibition effect of tween 80 surfactant is due to its physical adsorption on the magnesium surface.
- Upon integrating the whole theoretical data, it is obvious that w-branch plays the main role in the characteristics of tween 80. The uneven branching ratio is slightly more stable than even branched isomers. The physical adsorption site may originate from the magnesium HOMO to LUMO on the tween 80 that is localized on the ester group.

References

1. U.C. Nwaogu, C. Blawert, N. Scharnag, W. Dietze, K.U. Kainer, *Corros. Sci.*, 52 (2010) 2143.
2. El-Sayed M. Sherif, *Int. J. Electrochem. Sci.*, 6 (2011) 5372.
3. M. Hakamada, T. Furuta, Y. Chino, Y.Q. Chen, H. Kusuda, M. Mabuchi, *Energy*, 32 (2007) 1352.
4. Uan J-Y, Yu S-H, Lin M-C, Chen L-F, Lin H-I., *International Journal of Hydrogen Energy*, 34 (2009)6137.
5. Yu S-H, Uan J-Y, Hsu Tsang-Lin, *International Journal of Hydrogen Energy*, 37 (2012) 3033.
6. B.L. Mordike, *J. Mat. Proce. Tech.*, 117 (2001) 391.
7. Z. Xiaoqin, W. Quodong, L. Yizhen, Z. Yanping, D. Wenjiang, Z. Yunhu, *J. of Mat. Proce.Tech.*, 112 (2001) 17.
8. H. Friedrich, S. Schumann, *J. Mat. Proce. Tech.*, 117 (2001) 276.
9. N.A. El-Mahallawy, M.A. Taha, E. Pokora, F. Klein, *J. Mat. Proce. Tech.*, 73 (1998) 125
10. R.C. Zeng, J. Zhang, W.J. Huang, W. Dietzel, K.U. Kainer, C. Blawert, W. Ke, *Trans. Nonferrous Metal Society China*, 16 (2006) 763.

11. El-Sayed M. Sherif, *Int. J. Electrochem. Sci.*, 7 (2012) 4235
12. E.-S. M. Sherif, A.A. Almajid, *J. Appl. Electrochem.*, 40 (2010) 1555.
13. E.-S. M. Sherif, R.M. Erasmus, J. D. Comins, *J. Colloid. Inter. Sci.*, 311 (2007) 144.
14. A. Mesbah, C. Juers, F. Lacouture, S. Mathieu, E. Rocca, M. François, J. Steinmetz, *Solid State Sci.*, 9 (2007) 322.
15. X.H. Li, S.D. Deng, H. Fu, G. N. Mu, *Materials and Corrosion* 60 (2009)
16. M. Abdallah, A.Y. El-Etre, *Portugaliae Electrochimica Acta*, 21 (2003) 315
17. Gaussian 09, Revision D.01, Frisch, M. J.; Trucks, G. W.; Schlegel, H. B.; Scuseria, G. E.; Robb, M. A.; Cheeseman, J. R.; Scalmani, G.; Barone, V.; Mennucci, B.; Petersson, G. A.; Nakatsuji, H.; Caricato, M.; Li, X.; Hratchian, H. P.; Izmaylov, A. F.; Bloino, J.; Zheng, G.; Sonnenberg, J. L.; Hada, M.; Ehara, M.; Toyota, K.; Fukuda, R.; Hasegawa, J.; Ishida, M.; Nakajima, T.; Honda, Y.; Kitao, O.; Nakai, H.; Vreven, T.; Montgomery, J. A., Jr.; Peralta, J. E.; Ogliaro, F.; Bearpark, M.; Heyd, J. J.; Brothers, E.; Kudin, K. N.; Staroverov, V. N.; Kobayashi, R.; Normand, J.; Raghavachari, K.; Rendell, A.; Burant, J. C.; Iyengar, S. S.; Tomasi, J.; Cossi, M.; Rega, N.; Millam, N. J.; Klene, M.; Knox, J. E.; Cross, J. B.; Bakken, V.; Adamo, C.; Jaramillo, J.; Gomperts, R.; Stratmann, R. E.; Yazyev, O.; Austin, A. J.; Cammi, R.; Pomelli, C.; Ochterski, J. W.; Martin, R. L.; Morokuma, K.; Zakrzewski, V. G.; Voth, G. A.; Salvador, P.; Dannenberg, J. J.; Dapprich, S.; Daniels, A. D.; Farkas, Ö.; Foresman, J. B.; Ortiz, J. V.; Cioslowski, J.; Fox, D. J. Gaussian, Inc., Wallingford CT, 2009.
18. A. D. Becke, *J. Chem. Phys.*, 98(1993)5648.
19. C. Lee, W. Yang, R. G. Parr, *Phys. Rev. B*, 37(1988)785
20. S. H. Vosko, L. Wilk, M. Nusair, *Can. J. Phys.*, 58(1980)1200
21. S. Eid, M. Abdallah, E.M. Kamar, A.Y. El-Etre, *J. Mater. Environ. Sci.*, 6 (2015) 892
22. A. Ostovari, S.M. Hoseinie, M. Peikari, S.R. Shadizadeh, S.J. Hashemi, *Corros. Sci.*, 51 (2009) 1935
23. A. Zarrouk, B. Hammouti, H. Zarrok, S.S. Al-Deyab, M. Messali, *Int. J. Electrochem. Sci.*, 6 (2011) 6261 - 6274
24. F. M. Donahue, K. Nobe, *J. Electrochem. Soc.*, 112 (1965) 886.
25. E. Khamis, F. Bellucci, R. M. Latanision, E. S. H. El-Ashry, *Corrosion*, 47 (1991) 677.
26. G. Moretti, F. Guidi, G. Grion, *Corros. Sci.*, 46 (2004) 387.
27. N. O. Eddy¹, Femi Awe¹ and Eno E. Ebenso, *Int. J. Electrochem. Sci.*, 5 (2010) 1996
28. N. O. Eddy and Benedict I. Ita, *J Mol Model*, 17 (2011) 633
29. B. Ateya, B. El-Anadauli, F. El. Nizamy, *Corros. Sci.* 24 (1984) 509
30. Emranuzzaman, T. Kumar, S. Vishwanatham, G. Udayabhanu., *Corros. Eng. Sci. Technol.* 39 (2004) 327.
31. M.A. Deyab, S.S. Abd El-Rehim, *Int. J. Electrochem. Sci.*, 8 (2013) 12613
32. P. Udhayakala, T. V. Rajendiran, S. Gunasekaran, *J. Adv. Scient. Res.*, 3 (2012) 37.
33. Yahia H. Ahmad, Walid M. I. Hassan, *Int. J. Electrochem. Sci.*, 7 (2012) 12456
34. P. Udhayakala, T. V. Rajendiran, S. Gunasekaran, *J. Adv. Sci. Res.*, 3 (2012) 67